Penerbit Akademia Baru

Journal of Advanced Research in Fluid Mechanics and Thermal Sciences

Journal homepage: www.akademiabaru.com/arfmts.html
ISSN: 2289-7879

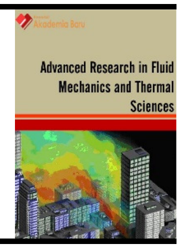

Rudimentary Effects of Emblematic Gust Excitations on the Lift Performance of Coaxial Helicopter Rotor Blades

Open Access

Ziad Abdul Awal[1], Mohd Shariff Ammoo[1], Shuhaimi Mansor[1], Iskandar Shah Ishak[1,*]

[1] Department of Aeronautical, Automotive and Ocean Engineering, Faculty of Mechanical Engineering, Universiti Teknologi Malaysia, 81310 Skudai Johor, Malaysia

ARTICLE INFO

Article history:
Received 25 February 2018
Received in revised form 13 March 2018
Accepted 7 April 2018
Available online 15 April 2018

Keywords:
Airflow, gust, helicopter, lift, main rotor

ABSTRACT

Aerodynamic valuation plays an imperative role in understanding the characteristic response of a helicopter with respect to the airflow. Understanding the airflow around the helicopter is much more challenging compared to the flow field around a fixed-wing aircraft. The situation becomes even more convoluted when environmental turbulences are introduced in the scene such as the gust wind loading, which is one of the most catastrophic commotions. Refereeing to the obvious, this study took out this daunting task to actually generate artificial gust and study its effects on the main rotor airflow physiognomies of a coaxially configured subscale helicopter. Quantitative data congregated by measuring the rotor induced airspeed underneath the rotor blades, which is quintessentially the lift/thrust, have revealed intriguing outcomes. The implementations of various strengths of active robust gust have caused the helicopter to experience half-hearted rolling motion pared with the incremental loss of altitude during hover. For forward flight, this investigation reveals the helicopter distinctively lost cruising speed along with the altitude as well when subjected to the gust. During hover and forward flight conditions, results depict that lift is decreased about 33% when subjected to the gust. These findings are alleged to be valuable for future research and development in the rotorcraft industry.

Copyright © 2018 PENERBIT AKADEMIA BARU - All rights reserved

1. Introduction

Experimental aerodynamic investigations remain the subject of interest in rotorcraft community since the flow around the helicopter is dominated by complex aerodynamics and flow interaction phenomena [1]. The radical breakthrough by the Wright brothers has revolutionized man's means of transportation and the aviation industry has been bourgeoning since then with cutting-edge designs, comprehensive ideas and nifty materials [2]. Irrefutably, modern aeronautical and aerospace engineering uncompromisingly demands for avant-garde materials along with astute designs [3]. Even though structural strength transpires to be an imperious portion in any aircraft design, for a rotorcraft the aerodynamics remains the most thought-provoking and abstruse impediment grappled by the aerodynamicists and designers even today [4]. The flow around a helicopter is dominated by

* *Corresponding author.*
E-mail address: shah@mail.fkm.utm.my (Iskandar Shah Ishak)

complex aerodynamics and flow interaction phenomena [5]. This is further elaborated by Wang and Zhao [6] stating that the rotor blades work at extraordinary serious unsteady environment compared with the fixed wing aircraft in normal forward flight and therefore its aerodynamic characteristics are more complex [6]. Due to its unique ability to hover along with other fundamental movements in any direction; rotorcrafts are becoming an essential need as its demand, expediency and usage are increasing rapidly [7]. As the main rotor makes an important contribution to the overall power consumption of the helicopter, modern rotors are optimized to have significant portions of laminar flow on the blades to ensure low drag [8].

Fundamentally, rotorcrafts in vertical flight are usually described by momentum theory and blade element theory. For a clear conception, the following sections describe these theories in a concise manner for general understanding.

1.1 Theory of Lifting Rotor
1.1.1 Momentum theory

Fundamentally, the momentum theory or otherwise known as the actuator disc theory is considered to be the simplest method that describes the lifting rotor [9]. It is fundamentally based on attaining a lifting force by generating a change of momentum. This theory assumes the presence of a stream-tube which is an axially symmetric surface passing through the rotor disc perimeter that isolates the flow though the rotor. Here, as the air is presumed to be incompressible; therefore, the flow past any cross-section of the stream-tube is constant. Furthermore, as the flow is one dimensional, the flow must remain in the same direction. This is appropriate for most flight conditions. On the other hand, this does give rise to a failing of the theoretical model under certain flight conditions. In the same way, after the flow enters the stream-tube, it is accelerated through the rotor disc and then exhausted from the bottom of the stream-tube. Further upstream of the disc, the vertical flow velocity tends to be zero which makes the stream-tube cross-section infinite in size. The stream-tube establishes itself as it passes through the rotor disc perimeter. It can be noted that, most of the models here are based on Glauert's theory of momentum transfer [10]. Referring to Figure 1, the additional velocity of V_i as it passes through the rotor is recognized as the induced velocity. It forms the wake with a velocity increase of V_2. The rotor thrust force, T, is evaluated by considering the momentum increase [9].

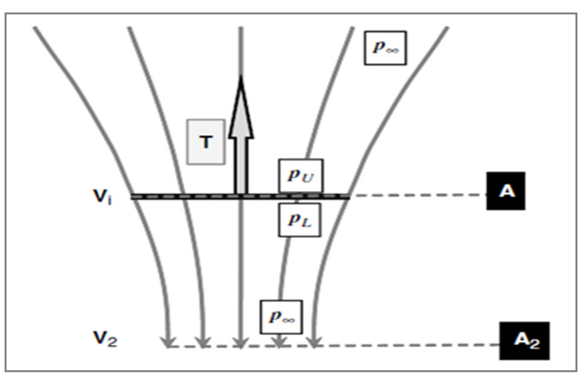

Fig. 1. Inflow air through rotor in hover [9]

The continuity of the flow through the stream-tube permits the following:

$$\rho A_1 V_1 = \rho A_2 V_2 \tag{1}$$

The rate of change of momentum gives the rotor thrust, therefore,

$$T = \rho A V_1 V_2 \tag{2}$$

The final deliberation is the addition of Bernoulli's equation. This equation is applied to the flow above or below the rotor disc, but not through it. Therefore, above the rotor,

$$P_\infty = P_U + \frac{1}{2}\rho V_i^2 \tag{3}$$

and below the rotor,

$$P_L + \frac{1}{2}\rho V_i^2 = P_\infty + \frac{1}{2}\rho V_2^2 \tag{4}$$

Now subtracting equation (4) and (3)

$$P_L - P_U = \frac{1}{2}\rho V_2^2 \tag{5}$$

Combining equation (2), (4) and (5) gives

$$V_2 = 2V_i \tag{6}$$

In other words, it can be said that the induced velocity gets doubled as the air forms the wake far downstream of the rotor. Combining (2) and (6) gives the following result,

$$V_i = \sqrt{T/2\rho A} = \sqrt{1/2\rho}\sqrt{T/A} \tag{7}$$

Equation (7) offers the link between disc loading and induced velocity. Disbursing of power is given by P_i, where this power is given a suffix of 'i' consistent with the induced velocity.
Therefore

$$P_i = TV_i \tag{8}$$

1.1.2 Blade element theory

According to Venkatesan [11], blade element theory is considered to be the grounds for most of the helicopter dynamics and aerodynamic analysis as it deals with the particulars of rotor system. Although, momentum theory is appropriate for predicting the rotor-induced velocity for a given rotor thrust; there are limitations when it comes to designing the rotor blades along with the entire rotor system. Nevertheless, there are a few imperative notions which require consideration. For a highly simplified case some of the assumptions are:

(i) The rotor blade is assumed to be rigid beam with no deformation
(ii) The rotor system rotates at a constant velocity Ω
(iii) The plane rotation for the rotor blades is perpendicular to the shaft
(iv) The rotor operates at a low disk loading
(v) Compressibility and stall effects are neglected

Figure 2 shows a typical cross section of the rotor blade where various velocity components and the resultant forces are acting on the airfoil section.

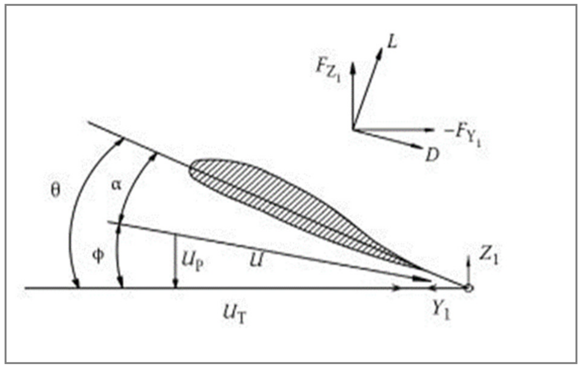

Fig. 2. Typical cross section of a rotor blade at radial location r and the velocity components [11]

In Figure 2, **θ** is the pitch angle for the blade which is measured from the plane of rotation. Subsequently, U_T and U_P are respectively the tangential and perpendicular relative air velocity components. In vertical flight, U_P is made up of velocity climb (VC) of the helicopter and the induced velocity (v). For hovering condition VC = 0 [11].

The relative air velocity components can be written as

$$U_T = \Omega_r \text{ and } U_P = VC + v \tag{10}$$

Now, the resultant air velocity U and the inflow angle are given by

$$U = \sqrt{\Omega_r^2 + (VC + v)^2} \tag{11}$$

and

$$\tan\phi = \frac{VC+v}{\Omega_r} \quad 12)$$

Also, the effective angle can be written as

$$\alpha = \theta - \phi \tag{13}$$

The sectional lift and drag forces can be written as

$$L = \frac{1}{2}\rho U^2 c C_l \tag{14}$$

and

$$D = \frac{1}{2}\rho U^2 c C_d \tag{15}$$

where c is the blade chord, C_d and C_l are the lift and drag coefficient, respectively. The equations can be used to resolve the two sectional forces along parallel and perpendicular directions to the rotor disk. The vertical and horizontal force components can be written as

$$F_{Z1} = \mathrm{L}\cos\phi - \mathrm{D}\sin\phi \tag{16}$$

$$-F_{y1} = \mathrm{L}\sin\phi - \mathrm{D}\cos\phi \tag{17}$$

Combining both equation (16) and (17) in thrust, torque and power element:

$$\mathbb{d}Q = -\mathrm{NF}_{Y1} r \mathbb{d}r \tag{18}$$

$$\mathbb{d}P = \Omega|dQ| = N|F_{Y1}|\Omega_r \mathbb{d}r \tag{19}$$

Subsequently, based on the assumptions solving even further will result in getting the thrust coefficient CT, torque coefficient CQ and power coefficient CP.

1.2 Research Motivation

According to Voogt and Doorn [12], helicopter accidents are predominantly dependent on different types of operation; where most fatal incidence during flights is associated to the weather. Referring to the statement, one such atmospheric occurrence is gust; where an abrupt and ephemeral proliferation in speed of the wind is demarcated as gust [13]. Congruently, according to Mashman [14], the most common cusses of turbulence and atmospheric phenomenon (which is also known as horizontal and vertical wind shear) faced by helicopter pilots include strong surface winds, gradient winds along with other variables. Besides, downdrafts and microbursts present a bigger threat to helicopters compared to fixed-wing aircrafts [14]. Therefore, understanding the effects of gust wind on helicopters is of great importance. Besides, the "vortex ring" of tail rotor in portside crosswind is weakened by the main rotor/tail rotor interaction, and the tail rotor thrust and unsteady air loads are significantly increased [15]. As the aerodynamics of rotorcraft in forward flight, particularly at high advance ratios, are highly complex [16], it is a demand to do the investigations. Be that as it may, significant research on helicopter main rotor air flow properties against active gusts is very inadequate. Despite a considerable effort by different companies, the Interactional Aerodynamic (I/A) problems remain a long dragged issue that adversely affected the overall performance, occupant comfort and handling qualities of helicopter [17]. The flow field around a helicopter is characterized by its inherent complexity including effects of fluid–structure interference, shock–boundary layer interaction, and dynamic stall [18]. It is dominated by complex aerodynamics and flow interaction phenomena [5]. This is due to the fact that conducting experiments on helicopters always transpire to be a daunting and expensive task. Although, numerical simulation is considered to be more advantageous when it comes to saving time and costs in comparison to conducting actual experiments [19] however, simulation results are never exact. Therefore, experimental models need to be scaled down in order reduce cost and other impediments. And so, this study took the liberty to artificially generate intrinsic gusts and implement them on a subscale helicopter in order to study the air flow physiognomies of the main rotor. The facts gathered from this study will essentially be constructive for improving helicopter performance against sudden gust wind and aid in avoiding grave catastrophes.

2. Methodology

2.1 Experimental Set-up

Experimental works have been recognised as well-testified instrumentation to conduct the research [20, 21]. The primary objective of this experimental investigation was to develop an artificial gust generating mechanism and see the effects of various strengths of gust on the main rotor of a subscale helicopter. Figure 3 depicts the final design of the gust generator.

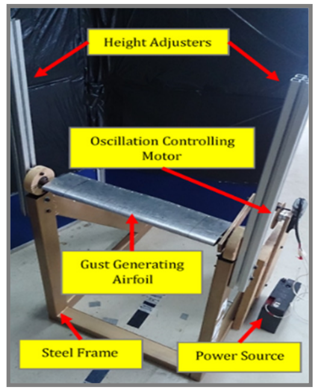

Fig. 3. Final design of the gust generator

It is basically a steel frame structure where a hollow aluminum sheet-bent airfoil is attached horizontally to this frame. This airfoil is capable of oscillating by the means of a motor at an average rate of 20 oscillations per 10 seconds. The gust generator is placed in front of the air blower where the airfoil's leading edge is faced towards the blower outlet. The principle behind doing this is that the air from the blower hits the oscillating airfoil's leading edge and then flows across the chord length to generate sinusoidal gusts through its trailing edge. A symmetrical airfoil (NACA0018) is utilized where it is postulated that due to its symmetric design, it will have an increasing chance of generating uniform sinusoidal gusts. The maximum pitch of the oscillating airfoil has been limited between +10^o and -10^o; because based on calculation, beyond this limit the airflow begins to stall gradually. Figure 4 shows the experimental set-up for this research investigation. Table 1 summarizes some fundamental features of the gust generator and table 2 summarizes the main rotor specifications.

2.2 Gust Strength Specification

Fundamentally, when the peak wind speed is no less than 16 knots (8.23 ms^{-1}) and the deviation of the peaks and lulls (or max and min) in wind speed is at least 9 knots (4.63 ms^{-1}), then it can be characterized as gusts. In general, the period of a gust should be under 20 seconds [13]. Based on these facts, three measures of gust strength starting from 8.3 ms^{-1} with an increment of 0.5 ms^{-1} until 9.3 ms^{-1} were selected for this investigation.

2.3 Data Collection Procedure

The quantitative data collection procedure is basically divided into two parts. The first one is quantifying the gust strength. This done by identifying the strength of the blower airspeed individually at various distances from the blower outlet in order to establish its functional range; after that the gust generator is placed in front of the blower where each of them work simultaneously to generate active sinusoidal gusts. Here, the generated gust is measured at variable distances from the airfoil's trailing edge. This is a vital part of the study as these results assists in identifying the exact position(s) to generate 8.3 ms^{-1}, 8.8 ms^{-1} and 9.3 ms^{-1} of gust. Subsequently, the second section of the study utilizes the generated gusts and implements them on the main rotor of the subscale helicopter. Figure 5(a) exemplifies the schematic diagram of the experimental set-up. Successively after finalizing all the prerequisites, the airspeed under the main rotor (in this case the lower rotor) is measured during both hover and forward flight for each strengths of gust. It can also be noted that, an anemometer is used to measure all the airspeed data for this investigative study. However, it is imperative to divide the measure points on rotor blade appropriately. During flight, the main rotor disk can be divided into three effective regions [22] namely “driving”, “driven” and “stall” regions which spans 45%, 30% and 25% respectively across the blade. Based on this theory, the blade is also divided into three sections where stall, driving and driven regions are allocated two equally divided measure points each. Figure 5(b) shows the airspeed measurement position(s) on the half-rotor blade span. For appropriateness, during data collection, the helicopter is viewed from the front during hover and from the side during forward flight. Further particulars are expounded in the subsequent sections.

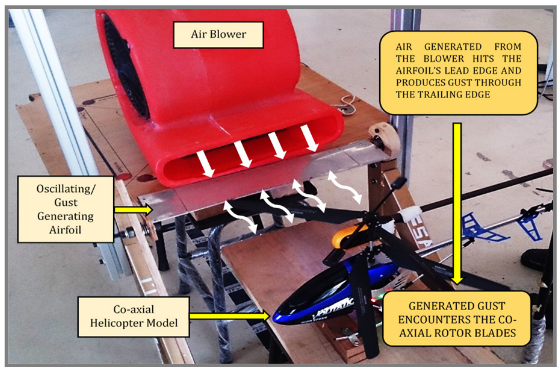

Fig. 4. Final experimental set-ups

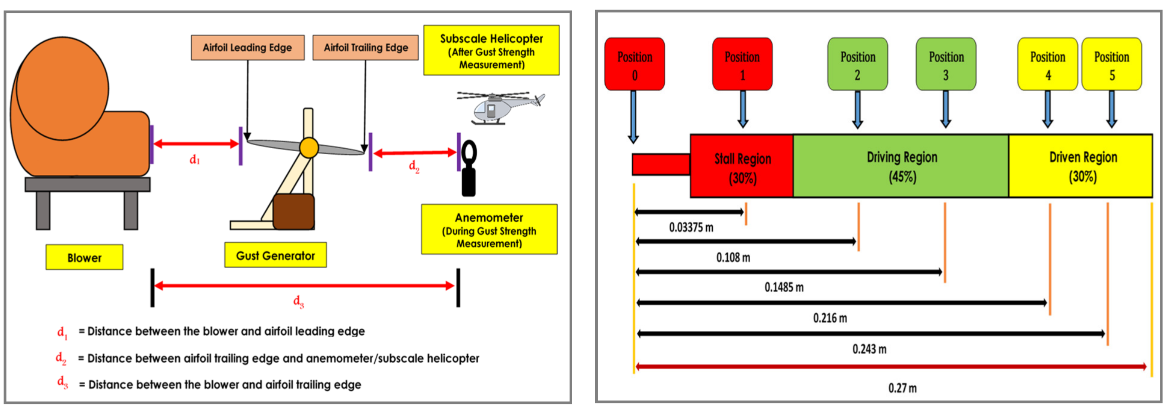

Fig. 5. (left) Schematic diagram of the experimental set-up (right) Airspeed measurement position(s) on the half-rotor blade span.

Table 1
Fundamental features of the gust generator

Motor	Mabuchi JC-578VA
No load speed	85 ± 15RPM
Rated Speed	60 ± 15RPM
Torque	2.9 Nm
Airfoil	NACA 0018
Span Length	0.5 m
Chord Length	0.1 m
Pithing Angular Limit	(+10°) to (- 10°)
Structure	Aluminum frame
Feature	Oscillating Airfoil with height adjusters

Table 2
Main rotor specifications

Rotor Configuration	Coaxial
Number of Blades	2+2
Rotor Blade Diameter	0.54 m
Type of Blades	Twisted

3. Results and Discussion

3.1 Generation of Active Sinusoidal Gusts

As the complete gust generating mechanism is a combination of the air blower and the gust generator, therefore the air speed range of the blower is identified at first. The graph in Figure 6 represents the air speed of the blower measured at an incremental distance from the outlet without the presence of the gust generator. It can be noticed that the airspeed has declined gradually with the expansion of distance from the blower outlet. Essentially, this graph abets in acquainting with the range of the blower which ensures whether it has the proficiency to generate the required gust strength of 8.3 ms^{-1}, 8.8 ms^{-1} and 9.3 ms^{-1} while retaining apposite space between the blower, the gust generator and the subscale helicopter. Subsequently, as mentioned earlier, the gust generator is placed in front of this blower where each of them functions simultaneously to generate active sinusoidal gusts.

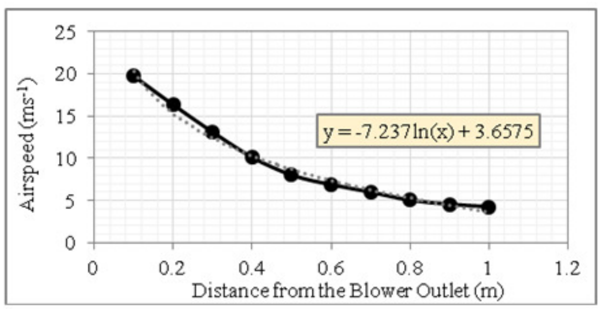

Fig. 6. Blower air speed against variable distance from blower outlet

The graphs in Figure 7 reveal the various strengths of gust being generated beginning at a distance of 0.1 m from the airfoil's trailing edge of the gust generator and moving further onwards until 0.8 m by an increment of 0.1 m. Essential specifies to be noticed here is the varying distance or gap in-between the blower, gust generator and anemometer. The first one is the gap between the blower and the airfoil's leading edge of the gust generator. The second one is the distance from the airfoil's trailing edge of the gust generator which could also be considered as the distance between the airfoil and anemometer. It can be perceived that the strength of gusts deteriorates as it moves further away from its origin or in this case the trailing edge of the airfoil. This gradual declining pattern remains true for each gap between the blower and airfoil. Suggestively, this graph assists in determining the required gap to generate gust strength of 8.3 ms^{-1}, 8.8 ms^{-1} and 9.3 ms^{-1} through interpolation/extrapolation. The helicopter is then placed at these positions where specified strengths of gust are being generated in order to study its effects on the main rotor.

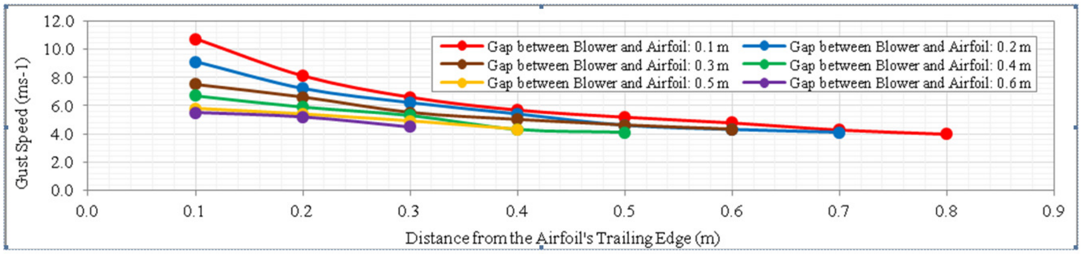

Fig. 7. Change of gust air speed against the distance from the airfoil's trailing edge of the gust generator

3.2 Airspeed underneath the main rotor

As mentioned beforehand, the airspeed is measured using an anemometer just underneath the lower rotor. It is imperative to comprehend the fact that this airspeed measured here is actually the blade induced airspeed. Basically, what transpires here is that the air gets sucked in by the rotor and directs the resultant induced air downwards at a higher velocity. This induced air, is in actual fact, the lift or thrust produced by the rotor blades. But for this case in point, instead of adhering to the conventional thrust evaluating procedure [23], this study distinctively utilizes the airspeed itself for quantifying the lift distribution on the rotor disk; this also provides an analogous relation (in terms of invariable units) with the gust strength as well. In this investigation, the airspeed underneath the main rotor blade is measured during both hover and forward flight condition for the case of 8.3 ms^{-1}, 8.8 ms^{-1} and 9.3 ms^{-1} of gust respectively. The following subsections present comparative analysis with respect to the normal and gusty condition for an in-depth understanding.

3.2.1 During hover

Figure 8 presents the graph of airspeed against the different span-wise positions on the main rotor during hover.

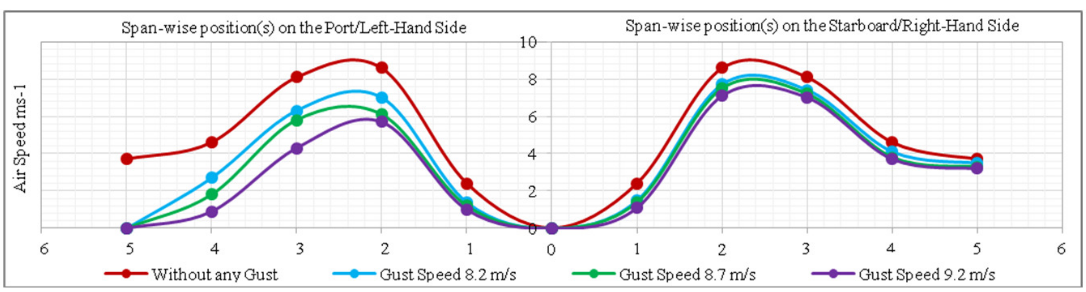

Fig. 8. Span-wise airspeed (or lift/thrust) distribution on the main rotor of the subscale helicopter for both with and without the manifestation of active gusts during hover

In this case, the subscale helicopter is viewed from the front and the active gusts are released from the left-hand side of the viewer's view point. In the graph, the data for normal condition is represented with the red colour line. On the other hand, blue orange and green coloured lines are for the case of 8.3 ms-1, 8.8 ms-1 and 9.3 ms-1 of gust respectively.

From Figure 8, it is evidently understood that in normal condition, the airspeed (or lift/thrust) is in poised condition on both right-hand side (starboard) and left-hand side (port). This is rather expected as the helicopter is in hovering state. As the positions on the blade have been demarcated earlier, the hub or the rotor center (Position 0) shows no sign of lift generation. Towards the end of the stall region there is a slight presence of lift; this lift on Position 1 carries on increasing gradually through the driving region reaching maximum value at Position 2. After that, the lift begins to decline around the stall region. This subsiding pattern carries on through Point(s) 3, 4 & 5. This pattern of lift distribution is identical on both the right and left-hand side of the main rotor during hover in normal atmospheric condition. However, this harmonic balance of lift gets disrupted when active gusts are introduced in scene. As gusts are released from the port or left-hand side, this transpires to be the most affected region. Form the graph, Point 5 on the port side of stall region shows no presence of lift for all the three strengths of gust. Although, there is the 'similar' increase pattern through Point(s) 1 & 2 followed by the gradual diminution through Point(s) 3 & 4; but the total lift (the area under the curve) produced is far less compared to normal condition without gust. This reduction in total lift is inversely proportional with the increasing strengths of gust. As the port side shows severe effect of the gust wind, the starboard side on the other hand displays a rather different scenario. Although, the 'typical' increase-decrease pattern of the lift distribution remains the same here, but the total lift under main rotor of the left-hand side reduces vaguely with the increasing gust. This can be rationalized with fact that this side is not directly struck by the gusts and is also away from the gust release zone. Above and beyond the fact that, increasing strengths of gust results in greater disparity in lift distribution. This disparity of lift distribution between both the sides of the rotor will eventually cause the helicopter to go through uneven half-pitched rolling motion along with the loss of altitude. In real-life condition, this incident could result in a very unpleasant flight or even cause the pilot to lose control depending the intensity of gust.

3.2.1 During forward flight

Figure 9 indicates the graph of airspeed against different span-wise positions on the main rotor during forward flight.

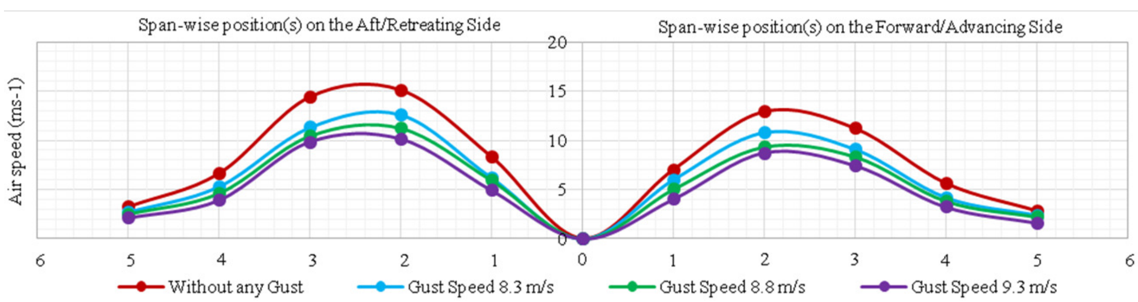

Fig. 9. Span-wise airspeed (or lift/thrust) distribution on the main rotor of the subscale helicopter for both with and without the manifestation of active gusts during forward flight

For this case the subscale helicopter is viewed from the side instead from the front like during hover. This is done in order to perceive the airspeed (or lift/thrust) distribution on the forward/advancing side and aft/retreating side of the main rotor. However, like before, the active gusts were again released from the left-hand side of the viewer's view point. Once again, the data for normal condition is differentiated with the red colored line along with 8.3 ms^{-1}, 8.8 ms^{-1} and 9.3 ms^{-1} of gust are sorted using blue, orange and green colored lines respectively. The graph evidently shows that in normal atmospheric condition, the lift distribution on the advancing and retreating side of the main rotor varies with each other during forward flight. This phenomena very much rational as it refers to the fact that the helicopter in forward motion. It can be noted that the lower rotor of the coaxial helicopter alters its pitch angel to generate more lift on the retreating side compared to the advancing side. As the rotor blades are continuously rotating, the variation in lift is maintained through the utilization of the swash plate. The variation in lift causes the lower main rotor to tilt and achieve forward motion. The cruising speed of the helicopter is controlled by altering the rotor rpm and the pitch angle. During forward flight, the rotor center (Position 0) remains inept in lift generation. In normal condition, although the retreating side has a higher total lift compared to the advancing side; the lift distribution pattern is rather similar to each other, where lift starts to increase through Position 1 and towards the end of the stall region which carries on increasing gradually through the driving region (including Position 2). After that, the lift begins to decrease around the stall region through Point(s) 3, 4 & 5. However, when gust is introduced during forward flight, the lift distribution on the main rotor exhibits docile behavior instead of a fitful one. Although the graph maintains the increase-decrease pattern, but with increasing gust, the total lift gradually declines on both advancing and retreating of the main rotor. The vital fact to be noticed here is the amount of total lift on the advancing and retreating side. As for forward motion requires having higher total lift on the retreating side compared to the advancing side; with a keen eye it can be noticed that with the increasing gust, the difference between the sides starts to reduce. This ominously points out the fact the in the helicopter will irrefutably lose cruising speed along with altitude due to the gust effect. This research findings are in good agreement with Linpeng stating that dynamic load due to gust for helicopter rotors directly affects the flight performance and it may cause the loss of trust force [24].

In real-life condition, loss of altitude could be counteracted by increasing the rotor rpm and pitch angel of the blades. However, maintaining the cruising speed would require the pilot to manually hold the tilting position strongly depending the intensity of gust.

4. Conclusion

This investigation intended to develop a mechanism in order to artificially generate active sinusoidal gusts and analyze its effects on the main rotor of a coaxial helicopter through understanding its configuration of the lift distribution. By doing so, intriguing results have been identified and are believed to be valuable for future research and development purposes. During hover and forward flight conditions, results depict that lift is decreased 32.56% and 33.33%, respectively, when subjected to the gust. Some of the imperative facts identified through this study are summarized as follows:

- During hover, active sinusoidal gusts have elicited the helicopter to experience hasty half- pitched rolling motion along with the slight loss of altitude. The rolling intensity and direction appears to be depended on the strength and the region of impact of the gust wind.
- During forward flight, active sinusoidal gusts have prodded the helicopter in losing cruising speed and altitude. This loss of cruising speed and altitude has appeared to be inversely related to the increasing strength of gust.

Acknowledgement

The authors would like to thank Mr. R. Rahim and Mr. K. Akif for their sincere effort along with Universiti Teknologi Malaysia (UTM) Helicopter Hanger for providing valuable technical support to conduct this research project. Authors were also indebted to Research University Grant (GUP) Tier 2 2017, Vot Number Q.J130000.2624.14J20.

References

[1] Ishak, Iskandar Shah, and Muhammad Fitri Mougamadou Zabaroulla. "EFFECTS OF HELICOPTER HORIZONTAL TAIL CONFIGURATIONS ON AERODYNAMIC DRAG CHARACTERISTICS." *JURNAL TEKNOLOGI* 79, no. 7-4 (2017): 67-72.

[2] Ammoo, M.S.B., Awal, Z.B.A. and Khairudin K.S. “Structural Analysis of UTM Single-Seat Helicopter Chassis”, *Jurnal Teknologi* 71, no. 2 (2014) 57-64.

[3] Awal, Ziad Bin Abdul, and Mohd Shariff bin Ammoo. "A Case Study on the Air Flow Characteristics of the Hirobo-FALCON 505 Controllable Helicopter's Main Rotor Blade." In *Applied Mechanics and Materials*, vol. 527, pp. 39-42. Trans Tech Publications, 2014.

[4] Ammoo, M. S. B., and Z. B. A. Awal. "An Investigation on Crack Alleviation in Bending of Aluminium 2024 for Aircraft Application." *International Journal of Research in Aeronautical and Mechanical Engineering* 2, no. 3 (2014): 255-269.

[5] Antoniadis, A. F., D. Drikakis, B. Zhong, G. Barakos, R. Steijl, M. Biava, L. Vigevano et al. "Assessment of CFD methods against experimental flow measurements for helicopter flows." *Aerospace Science and Technology* 19, no. 1 (2012): 86-100.

[6] Wang, Qing, and Qijun Zhao. "Modification of Leishman–Beddoes model incorporating with a new trailing-edge vortex model." *Proceedings of the Institution of Mechanical Engineers, Part G: Journal of Aerospace Engineering* 229, no. 9 (2015): 1606-1615.

[7] Ammoo, M.S.B., Awal, Z.B.A. and Sangiti N.M. "Static and Dynamic Balancing of Helicopter Tail Rotor Blade Using Two-Plane Balancing Method". *Jurnal Teknologi* 71, no. 2 (2014) 49-55.

[8] Richter, Kai, Stefan Koch, Andreas Goerttler, Benjamin Lütke, Christian C. Wolf, and Andreas Benkel. "Unsteady boundary layer transition on the DSA-9A rotor blade airfoil." In *41st European Rotorcraft Forum, Munich, Germany*, pp. 1-4. 2015.

[9] Seddon, John M., and Simon Newman. *Basic helicopter aerodynamics*. Vol. 40. John Wiley & Sons, 2011.

[10] Glauert, Hermann. *The elements of aerofoil and airscrew theory*. Cambridge University Press, 1983.

[11] Venkatesan, C. *Fundamentals of helicopter dynamics*. CRC Press, 2014.

[12] Voogt, A. de, and Robert RA van Doorn. "Helicopter accidents: data-mining the NTSB database." (2007).

[13] Wind Gust (Definition). "National Oceanic and Atmospheric Administration-NOAA". National Weather Service, Dept. of Commerce US. 2017. Web-link: http://graphical.weather.gov/definitions/defineWindGust.html

[14] Mashman, Joe. "Helicopters and turbulence." *Hospital Aviation* 8, no. 7 (1989): 34-35.

[15] Tan, J. "Influence of Helicopter Rotor on Tail Rotor Unsteady Aerodynamic Loads". *Acta Aeronautica et Astronautica Sinica*. Vol. 36 Issue (10): 3228-3240

[16] Hodara, Joachim, and Marilyn J. Smith. "Improvement of crossflow aerodynamic predictions for forwarded flight at all advance ratios." (2014).

[17] de Ward, P. G., and M. Trouvé. "Tail Shake Vibration: Objective Comparison of Aerodynamic Configurations in a Subjective Environment." *1999.* (1999).

[18] De Gregorio, Fabrizio. "Flow field characterization and interactional aerodynamics analysis of a complete helicopter." *Aerospace Science and Technology* 19, no. 1 (2012): 19-36.

[19] Abdul Awal, Ziad Bin, and Mohd Shariff bin Ammoo. "Numerical Simulation and Investigation of Transonic & Symmetrical Airfoil for Helicopter Main Rotor Blade Application." *Applied Mechanics & Materials* 704 (2014).

[20] Md Nizam Dahalan, Ahmad Fitri Suni, Iskandar Shah Ishak, Nik Ahmad Ridhwan Nik Mohd, Shabudin Mat, "Aerodynamic Study of Air Flow Over A Curved Fin Rocket", *Journal of Advanced Research in Fluid Mechanics and Thermal Sciences* 40, no 1 (2017): 46-58.

[21] Kasim, K.A., Mat S., Ishak, I.S. and Said, M. "Effects of Propeller Locations on the Vortex System Above Delta-Shaped UAV Model", 30th Congress of The International Council of the Aeronautical Sciences, ICAS 2016, Document ID 9783932182853.

[22] Ammoo, M. S. B., and Z. B. A. Awal. "Main Rotor Blade Air Flow Characteristics & Behaviour of a Remote Controlled Sub-scale Helicopter: A Case Study." *International Journal of Research in Aeronautical and Mechanical Engineering* 1, no. 7 (2013): 228-235.

[23] Awal, Ziad Bin Abdul, M. S. B. Ammoo, and N. S. B. Jamaluddin. "The Effect of Rotor Disc Clearance on the Lift Performance of Contra-Rotating Rotor Blades." *International Journal of Research in Engineering and Technology* 3, no. 5 (2014): 739-745.

[24] Wang, Linpeng, Yuting Dai, and Chao Yang. "Gust Response Analysis for Helicopter Rotors in the Hover and Forward Flights." *Shock and Vibration* 2017 (2017).